ANALYSIS OF PICOSECOND LASER-INDUCED FLUORESCENCE PHENOMENA IN PHOTOSYNTHETIC MEMBRANES UTILIZING A MASTER EQUATION APPROACH

G. PAILLOTIN, C. E. SWENBERG, J. BRETON, and N. E. GEACINTOV, *Service de Biophysique, Département de Biologie, Centre d'Etudes Nucléaires de Saclay, BP 2, 91190 Gif-sur-Yvette, France*

ABSTRACT   A Pauli master equation is formulated and solved to describe the fluorescence quantum yield, ϕ, and the fluorescence temporal decay curves, $F(t)$, obtained in picosecond laser excitation experiments of photosynthetic systems. It is assumed that the lowering of ϕ with increasing pulse intensity is due to bimolecular singlet exciton annihilation processes which compete with the monomolecular exciton decay processes; Poisson statistics are taken into account. Calculated curves of ϕ as a function of the number of photon hits per domain are compared with experimental data, and it is concluded that these domains contain at least two to four connected photosynthetic units (depending on the temperature), where each photosynthetic unit is assumed to contain ~ 300 pigment molecules. It is shown that under conditions of high excitation intensities, the fluorescence decays approximately according to the $(\text{time})^{1/2}$ law.

INTRODUCTION

It is now generally accepted that bimolecular exciton interactions occur in photosynthetic membranes when intense laser excitation sources are employed. When a single picosecond laser pulse is used for excitation of the fluorescence, singlet-singlet exciton annihilation is dominant. However, when a pulse sequence or microsecond duration excitation pulses are employed, annihilation of singlet excitons by triplet excitons is important (1-3). Experimentally, exciton annihilation manifests itself by a decrease in the lifetime of the fluorescence (4) and by a decrease in the integrated quantum yield of fluorescence, ϕ, as the intensity I of the excitation is increased (5-7).

   Two different models have been proposed to account for the shape of the ϕ vs. I curves. Mauzerall (6, 7) was the first to account for the decrease in the fluorescence quantum yield by utilizing Poisson distributions of photon hits per domain which contained up to four reaction centers. Swenberg et al. (8) proposed a continuous model kinetic equation to describe exciton annihilation by standard bimolecular rate equations, which was used by Geacintov et al. (9) to fit their ϕ vs. I curves at four different temperatures.

   In this paper, utilizing a standard Pauli master equation approach, a general theory of bimolecular exciton processes in confined domains is developed. No assumptions concern-

---

ing the dimensions of the domains are made in this theory, but the minimum dimensions of such domains can be estimated by comparing theoretically calculated and experimentally obtained ϕ vs. I curves. This theory takes into account the statistics of photon hits in an ensemble of microscopic domains and can also be used to interpret the shapes of fluorescence decay curves after picosecond laser excitation. It is shown that the Swenberg case (8) is obtained when the unimolecular singlet exciton decay rate is much larger than the singlet-singlet annihilation rate. A detailed comparison between this model of fluorescence quenching and the one proposed by Mauzerall (6, 7) is given.

It is also shown that this theory can account for the $\sqrt{t}$ fluorescence decay law observed by Porter and his co-workers (10–14) when intense picosecond laser pulses are used for excitation.

This theory of exciton annihilation in photosynthetic domains is characterized by the following assumptions and considerations: (a) the exciton distribution randomization time, τ_R, is very short and is smaller than the characteristic exciton annihilation time τ_A; (b) the depletion of ground state molecules is considered to be negligible; this assumption is justified within most of the intensity ranges studied (9); (c) the exciton coherence time, τ_C, is extremely short, so that memory effects can be neglected (15); theoretical investigations provide evidence that τ_C is less than 10^{-13} s so that random hopping-like motion of excitation energy in the photosynthetic pigment system constitutes an adequate description of the energy transfer process (16).

The theory developed here is consistent with all of the known experimental data and can be utilized to estimate the number of connected photosynthetic units per domain and the bimolecular annihilation rate constants in photosynthetic membranes. It is shown that the lake model is a more appropriate description of the photosynthetic membrane than the puddle model (17).

EXCITON DECAY PROCESSES IN PHOTOSYNTHETIC DOMAINS

We consider a domain consisting of M chlorophyll molecules. A picosecond flash creates i excitons within this domain, and these excitons decay in time by nonradiative and by radiative (fluorescence) processes.

At sufficiently low excitation intensities only one exciton is created per domain. Under these conditions ($i = 1$), the exciton decays by the usual monomolecular processes, characterized by the rate constant K, where
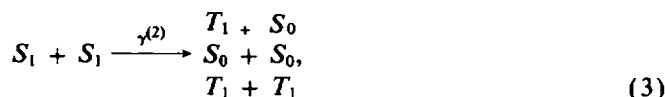
$$K = k_F + k_{IS} + k_D + k_Q. \tag{1}$$

k_F is the radiative decay constant, k_{IS} is the intersystem crossover rate constant, k_D is a nonradiative term characterizing the decay from the S_1 (first excited singlet) to the ground state S_0, whereas k_Q denotes the quenching of S_1 by the reaction centers. This latter term normally depends on the state of the reaction center (18). In this paper our attention is confined to the case of closed reaction centers; changes in k_Q due to previous interaction with an exciton are not considered. This theory is therefore limited to the type of picosecond laser pulse fluorescence quenching experiments in which the reaction centers are closed, e.g., by a continuous background illumination (9). In general, the set of pigments associated with such a reaction center is called a photosynthetic unit (PSU). In green plants a PSU contains

about 300 chlorophyll molecules. Numerous lines of evidence indicate that the PSUs are not isolated (19, 20) but are grouped in domains (see also references 6 and 7). In our terminology there are d photosynthetic units per domain, where each domain contains a total of M chlorophyll molecules.

When several excitons are created simultaneously in a given domain, bimolecular exciton-exciton annihilation processes are possible. It is assumed that excitons in different domains cannot interact with each other. When the initial exciton density is not too large (less than 1 exciton per 10 pigment molecules, for instance), the simultaneous encounter and annihilation of more than 2 excitons at one time is considered to be negligible.

When picosecond pulses are used for excitation, the major bimolecular deactivation process is believed to be singlet-singlet annihilation (21). Singlet-triplet annihilation does not play an important role (2). Singlet-singlet exciton annihilation may lead to the disappearance of either one (Eq. 2) or both excitons (Eq. 3):

$$S_1 + S_1 \xrightarrow{\gamma^{(1)}} S_1 + S_0 \tag{2}$$

$$S_1 + S_1 \xrightarrow{\gamma^{(2)}} \begin{array}{l} T_1 + S_0 \\ S_0 + S_0, \\ T_1 + T_1 \end{array} \tag{3}$$

where T_1 represents the lowest triplet state, and $\gamma^{(1)}$ and $\gamma^{(2)}$ denote the appropriate bimolecular rate constants. For our purposes, the exact nature of the final states, i.e., the relative probabilities of the three different channels in Eq. 3, need not be considered.

FORMULATION OF THE MASTER EQUATION

A rigorous treatment of singlet-singlet annihilation in a domain requires the solution of a multidimensional diffusion equation. Formally, one must solve a connected set of spatial distribution function equations. We shall adopt the uniform or random approximation, which allows us to neglect the spatial variables. This approximation is valid when L_0, the mean diffusion length of the singlet exciton, is much greater than the average separation, δr, between excitons, i.e., $L_0 \gg \delta r$. This approximation is equivalent to assuming that the exciton spatial distribution is randomized within a time interval that is small compared with the characteristic bimolecular and monomolecular decay times (16, 22).

With this assumption, the state of a domain is defined by the number (i) of excitons it contains at any particular time interval t after the incidence of the picosecond excitation pulse at $t = 0$. In a domain excitons may either appear or disappear in time due to mono- and bimolecular rate processes. These processes are depicted schematically in Fig. 1. A state with i excitons may disappear to give rise to an ($i - 2$) state by the bimolecular process described above (Eq. 3), or to an ($i - 1$) state by the monomolecular (Eq. 1) or bimolecular processes (Eq. 2). Similarly, a state with i excitons may appear because of the decay of ($i + 1$) and ($i + 2$) states, as shown in Fig. 1.

The rate of decay of the i-state by the monomolecular process is given by

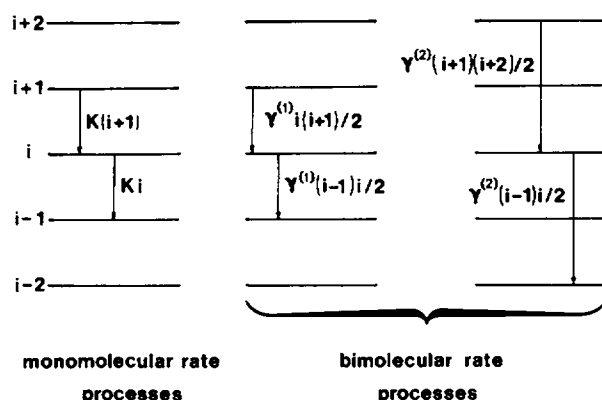$$T^{(\text{mono})}(i \rightarrow i - 1) = Ki. \tag{4}$$

FIGURE 1   Definition of kinetic exciton deactivation processes. The symbols $i, i + 1, i - 1$, etc. define the state of the domain containing $i, i + 1, i - 1$, etc. excitons. K is the monomolecular decay constant; $\gamma^{(1)}$ and $\gamma^{(2)}$ are bimolecular exciton annihilation constants resulting in the disappearance of only one or of both singlet excitons per annihilation event.

The rate of decay of the i-state by bimolecular processes is given by

$$T^{(\alpha)}(i \rightarrow i - \alpha) = \gamma_{12}^{(\alpha)} + \gamma_{13}^{(\alpha)} + \cdots + \gamma_{1i}^{(\alpha)} + \gamma_{23}^{(\alpha)} + \gamma_{24}^{(\alpha)} + \cdots$$

$$= \sum_{k=1}^{i} \sum_{l=k+1}^{i} \gamma_{kl}^{(\alpha)}. \tag{5}$$

The index $\alpha = 1$ or 2, depending on the mode of bimolecular annihilation (either Eq. 2 or 3, respectively). In general, the bimolecular rates $\gamma_{kl}^{(\alpha)}$ depend on the positions of the kth and lth excitons. However, if we define

$$\gamma_p^{(\alpha)} = \frac{1}{M} \sum_{q=1}^{M} \gamma_{pq}^{(\alpha)}, \tag{6}$$

where M denotes the total number of sites (molecules) within a domain; if we assume complete randomization of the spatial exciton distribution, as discussed above, Eq. 5 simplifies to read:

$$T^{(\alpha)}(i \rightarrow i - \alpha) = \tfrac{1}{2} i(i - 1) \gamma^{(\alpha)} \tag{7}$$

where

$$\gamma^{(\alpha)} = \frac{1}{M} \sum_{n=1}^{M} \gamma_n^{(\alpha)}. \tag{8}$$

Under these conditions, where the quenching of singlet excitons by triplets is completely neglected and a delta function source of excitation is employed, the Pauli master equation is

$$dp_i(n, t)/dt = T^{(mono)}(i + 1 \rightarrow i)p_{i+1}(n, t) + \sum_{\alpha = 1,2} T^{(\alpha)}(i + \alpha \rightarrow i)p_{i+\alpha}(n, t)$$

$$- T^{(mono)}(i \rightarrow i - 1)p_i(n, t) - \sum_{\alpha = 1,2} T^{(\alpha)}(i \rightarrow i - \alpha)p_i(n, t), \quad (9)$$

and, according to Eqs. 4 and 7:

$$dp_i(n, t)/dt = K(i + 1)p_{i+1}(n, t) + \gamma^{(1)} \frac{i(i + 1)}{2} p_{i+1}(n, t) + \gamma^{(2)} \frac{(i + 1)(i + 2)}{2}$$

$$p_{i+2}(n, t) - \left(Ki + \gamma^{(1)} \frac{i(i - 1)}{2} + \gamma^{(2)} \frac{i(i - 1)}{2}\right) p_i(n, t). \quad (10)$$

In these equations, $p_i(n, t)$ is the probability that at time t there are i excitons in a given domain, when at $t = 0$ there were n excitons in this domain created by the delta function excitation. The physical significance of these equations (9 and 10) may be clarified by considering the average number of excitons, $<i>$, in a domain at time t:

$$<i> = \sum_{i=1}^{n} ip_i(n, t). \quad (11)$$

Performing the appropriate summations over each term in Eq. 10 gives

$$\frac{d<i>}{dt} = - K<i> - \left(\gamma^{(2)} + \frac{\gamma^{(1)}}{2}\right) <i(i - 1)>. \quad (12)$$

If the domain is considered to be sufficiently large so that the exciton density can be treated as a continuous variable, then $<i(i - 1)> \simeq <i>^2$. In this case, Eq. 12 reduces to the standard bimolecular rate equation for the disappearance of excitons (23), used by Swenberg et al. (8) to describe the fluorescence quenching in the PSU at high excitation intensities.

CALCULATION OF THE EXPERIMENTAL OBSERVABLES $F(t)$ AND ϕ

In a domain in which n excitons were created at $t = 0$, the intensity of fluorescence $F_n(t)$ is given by the equation:

$$F_n(t) = \frac{1}{n} \sum_{i=1}^{n} ip_i(n, t). \quad (13)$$

This intensity is normalized to unity at $t = 0$, so that $F_n(0)$ equals unity.
For such a domain the integrated quantum yield of fluorescence is given by:

$$\phi_n = k_F \int_0^\infty F_n(t)dt. \quad (14)$$

In an actual experiment, there are many domains, each of which may have absorbed a different number of photons. It is thus only possible to determine experimentally a mean number y of exciton created per domain. It is convenient to introduce the probability that a given domain contains n excitons at $t = 0$. This probability is given by a Poisson distribu-

tion. The macroscopically measurable fluorescence intensity is thus:

$$F(t) = \frac{1}{y}\sum_{n=0}^{\infty} \frac{y^n e^{-y}}{n!}(nF_n(t)) = \sum_{n=1}^{\infty} \frac{y^{n-1}e^{-y}}{(n-1)!}F_n(t). \tag{15}$$

Similarly, the measured fluorescence quantum yield is:

$$\phi = k_F \int_0^{\infty} F(t)dt = \sum_{n=1}^{\infty} \frac{y^{n-1}e^{-y}}{(n-1)!}\phi_n. \tag{16}$$

The evaluation of these two quantities, $F(t)$ and ϕ, requires that the Pauli equation (Eq. 10) be solved. This solution, and the calculation of $F_n(t)$ in Eq. 15, are outlined in the Appendix.

We introduce the following parameters:

$$\gamma = \gamma^{(1)} + \gamma^{(2)}, \quad r = 2K/\gamma, \quad \xi = \gamma^{(2)}/\gamma, \quad Z = y(1 + \xi). \tag{17}$$

γ is the overall "rate of decay" by singlet-singlet annihilation of a given pair of excitons. We further note that for this pair of excitons, the rate of decay by monoexcitonic processes is equal to $2K$. It is thus evident that r is a dimensionless parameter, because it is a ratio of these two rates.

According to Eq. A-21, $F(t)$ can be described by a sum of exponentials:

$$F(t) = \sum_{p=0}^{\infty} (-1)^p \exp[-(p+1)(p+r)\tau]A_p, \tag{18}$$

where

$$A_p = \sum_{k=p}^{\infty} \frac{(-1)^k k! Z^k (r+1+2p)}{p!(k-p)!(r+p+1)\cdots(r+p+1+k)} \tag{19}$$

with $\tau = \gamma t/2$.

Using Eq. A-21 again, we obtain

$$\phi = \phi_0 r \sum_{k=0}^{\infty} (-1)^k \frac{Z^k}{r(r+1)\cdots(r+k)}\frac{1}{k+1} \tag{20}$$

where $\phi_0 = k_{F/K}$ is the fluorescence quantum yield in the low excitation intensity limit.

Before proceeding to explicit calculations of $F(t)$ and of ϕ as a function of the average number of photon hits per domain, we shall consider two limiting cases.

THE LIMITING CASES OF $r \to 0$ AND $r \to \infty$

Because r is defined as being equal to $2K/\gamma$, $r \to \infty$ implies that the "rate" of bimolecular annihilation $\gamma \ll 2K$, i.e., is much smaller than the monomolecular decay rate. This type of situation occurs when the dimensions of the domains are large. In the case $r \to \infty$, the last term on the right-hand side of Eq. A-19 is negligible and, after integration, we obtain:

$$F(t) = 1/[e^{Kt}(1 + Z/r) - Z/r]. \tag{21}$$

This result is in agreement with the analogous quantity $F(t)$ derived from standard bimolecular kinetics (8). The quantum yield for this case is

$$\phi = \frac{k_F}{Z} \int_0^\infty F(t)dt = \phi_0 \frac{r}{Z} \ln\left(1 + \frac{Z}{r}\right).$$ (22)

This equation, a function of the dimensionless variables Z and r, is similar to the one utilized by Swenberg et al. (8, 9). These dimensionless variables are transformed to the analogous constants used in standard bimolecular kinetic theories by introducing the surface S of these domains:

$$Z/r = (Z/2K)\gamma = (Z/S) \cdot \gamma S \cdot 1/2K.$$ (23)

Z/S thus has the dimensions of an exciton density, whereas γS has the dimensions of a diffusion constant.

In the opposite limit when r is small, i.e., when $\gamma \gg 2K$,

$$F(t) = \frac{1 - e^{-Z}}{Z} e^{-Kt} \qquad \text{for} \qquad t \neq 0,$$ (24)

whereas for $t = 0$, $F(0) = 1$.

At $t = 0$, the fluorescence yield drops rapidly to the value $(1 - e^{-Z})$. For $t > 0$, the normal, low intensity limit exponential decay time is observed.

The time dependence of the fluorescence intensity, $F(t)$, in the two limiting cases of $r \to 0$ and $r \to \infty$ is depicted schematically in Fig. 2.

The quantum yield of fluorescence in the $r \to 0$ case is:

$$\phi = \phi_0(1 - e^{-Z})/Z.$$ (25)

This equation is similar to the one obtained by Mauzerall (7) for the case of closed reaction centers, which he used in his analysis of the quenching of the prompt fluorescence in photosynthetic systems. The similarities and differences between the model of fluorescence quenching presented here and the model proposed by Mauzerall (6, 7) are discussed in more detail below.

THE TIME DEPENDENCE $F(t)$ OF THE FLUORESCENCE DECAY AND THE $\sqrt{t}$ DECAY LAW

The general expression for the fluorescence decay profile after a delta function excitation pulse is given by Eqs. 18 and 19. We expand the first few terms of the series in Eq. 18 to give

$$F(t) = A_0(Z, r)e^{-Kt} - A_1(Z, r)e^{-(r+1)\gamma t} + A_2(Z, r)e^{-\frac{1}{2}(2+r)\gamma t}$$
$$- A_3(Z, r)e^{-2(r+3)\gamma t} + \cdots . \quad (26)$$

The preexponential factors are seen to depend on the average number of hits per domain $[Z = y(1 + \xi)]$ and the ratio of bimolecular to unimolecular rate constants, r. The decay is thus represented by a sum of weighted exponentials. The first term in the series is the low-intensity decay term and as $Z \to 0$, $A_0 \to 1.0$, whereas all other terms $A_p(p \neq 0) \to 0$, as expected. Furthermore, all of the terms $A_p(p \neq 0)$ decay faster than the A_0 term; thus, the final portion of the decay curve should always display the normal exponential Kt com-
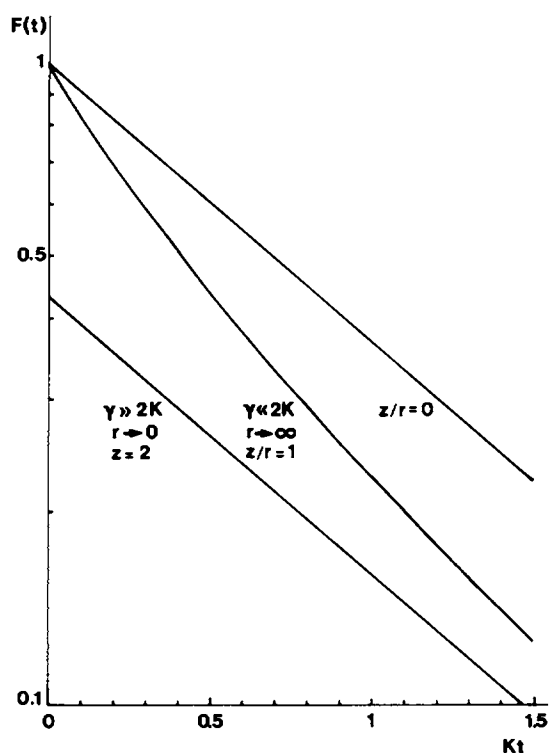
FIGURE 2 The time dependence of the fluorescence $F(t)$ after a delta function excitation pulse at $t = 0$ for the two limiting cases $r = 0$ and $r = \infty$. For $r = 0$ the parameter Z, proportional to the number of hits per domain, was arbitrarily taken to equal 2. For r large the ratio Z/r was taken to equal 1. The upper curve represents the exponential decay for the low intensity case $Z/r \rightarrow 0$.

ponent observed at low pulse intensities. Physically, this situation arises because there is a finite possibility that there is only one last exciton within the domain, regardless of how many were there initially.

The temporal profile of the fluorescence decay profiles thus depends in a complicated manner on the values of Z and r. Examples of typical decay curves calculated according to Eqs. 18 and 19 using $Z = 10$ and different values of r are shown in Figs. 3 A and B.

In general, it is difficult to compare experimental fluorescence decay curves with the theoretical expressions, Eqs. 18, 19, and theoretical fits to data are generally feasible only in the limiting cases described by Eqs. 20 and 24. However, it can be shown that

$$\frac{d}{dt} \text{Ln}\,(F(t))\bigg|_{t=0} = K + \gamma/2Z \qquad (27)$$

$$\frac{d}{dt} \text{Ln}\,(F(t))\bigg|_{t \rightarrow \infty} = K. \qquad (28)$$

The ratio of these two equations is just $(1 + Z/r)$. In theory, therefore, it is possible to estimate r from the limiting asymptotic slopes of the $F(t)$ curve and from a knowledge of z.

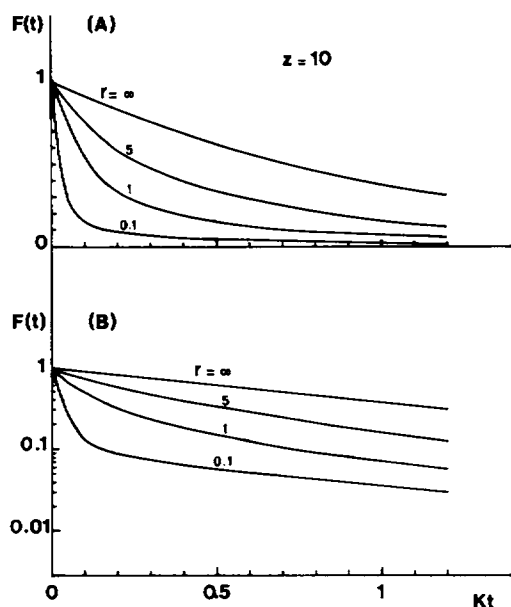Recently, Beddard and Porter (11), Searle et al. (12), and Harris et al. (13) have reported

FIGURE 3   The time dependence after a delta function excitation pulse at $t = 0$ for the general case $0 < r < \infty$, calculated according to Eq. 26, utilizing Z (proportional to the number of hits) $= 10$ and different values of r:0.1, 1,2,5. (A) Linear fluorescence intensity $F(t)$ scale; (B) logarithmic $F(t)$ scale.

that experimentally determined fluorescence decay curves after excitation with picosecond laser pulses obey the decay law

$$\ln\{F(t)\} \propto - A\sqrt{t},\qquad (29)$$

where A is a constant.

In Fig. 4 we have plotted $\ln\{F(t)\}$ as a function of $\sqrt{t}$ where $F(t)$ was calculated from Eqs. 18 and 19 for various values of r, and $Z = 10$. It is evident that the $r = 2$–5 curves for $Z = 10$ resemble the empirical $\sqrt{t}$ decay law as described by Eq. 29. This result illustrates that the theory developed here encompasses the $\sqrt{t}$ decay law observed by others (11–13) for high intensities and for selected values of the parameter r. At low excitation intensities, however, our theory predicts that the fluorescence decay is strictly exponential. Barber et al. (17), using relatively low intensity picosecond laser pulse excitation, have apparently observed a $\sqrt{t}$ decay law even for small Z. This experimental result was rationalized in terms of the Förster decay law (24). This decay law was derived by Förster for the case of energy transfer from a donor, D^*, to a set of acceptor molecules, A, spaced at variable distances, R_n, from the donor. The decay of the electronically excited donor molecules, D^*, is given by

$$dD^*/dt = - kD^* - \sum_n k_n D^*.\qquad (30)$$

The summation is carried out over all acceptor molecules n in the vicinity of D^*. The rate constant k_n depends on the concentration of acceptor molecules and on the distribution of distances R_n between D^* and A. The $\sqrt{t}$ decay law is obtained by averaging over all possible distances R_n in three-dimensional space and assuming the usual Förster R_n^{-6}
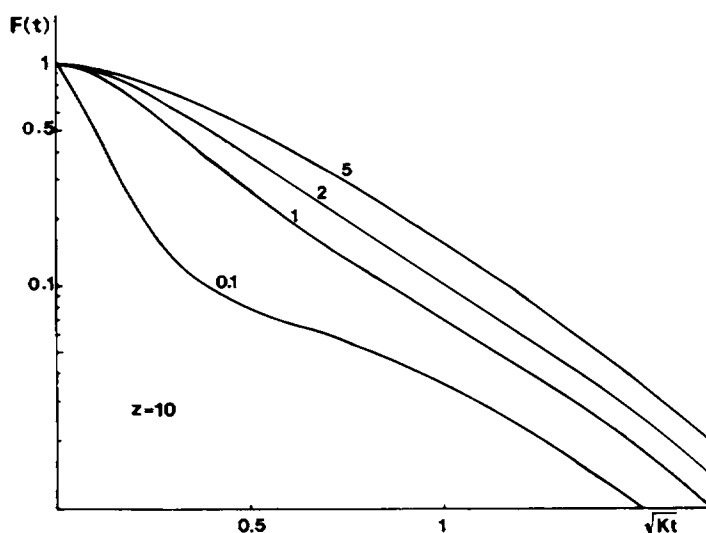
FIGURE 4 The fluorescence intensity, $F(t)$, plotted as a function of the square root of the time, utilizing Eq. 26 for different values of the parameter r.

distance dependence $(k_n \propto (R_0/R_n)^6)$. In two- and one-dimensional space, the decay laws $F(t) \propto - t^{1/3}$ and $F(t) \propto - t^{1/6}$ are obtained. These spatial averages presume that k_n in Eq. 30 and thus the acceptor concentration and distances R_n remain constant in time. These assumptions are unrealistic in the case of singlet-singlet annihilation because neither R_n nor the concentration of quenchers remains constant in time.

We thus conclude in accord with Knox (22) that the Förster theory is not an adequate theoretical description of fluorescence decay profiles obtained in picosecond laser excitation experiments. A $\sqrt{t}$ decay law can, on the other hand, be obtained from solutions of the master equation presented here. The only basic assumption inherent in this theory is the neglect of spatial variables in the description of the dynamics of singlet excitons on the time scale of 10^{-11}–10^{-9} s. This time scale corresponds to the time domain in which fluorescence decay curves have been measured to date.

INTEGRATED FLUORESCENCE YIELD, ϕ, AS A FUNCTION OF PULSE INTENSITY

In using Eq. 20 to evaluate ϕ, it was found convenient to use the recurrence relation

$$\phi(y, r) = \frac{(r - 1)!(-1)^{r-1}}{y^r} \left\{ e^{-y} - \sum_{k=0}^{r-1} \frac{(-1)^k y^k}{k!} + \frac{r}{r-1} \phi(y, r-1) \right\}, \quad (31)$$

in which we have made the further simplifying assumption that $y = Z$ (i.e., $\xi = 0$, which is equivalent to $\gamma^{(2)} = 0$). Without this simplifying assumption, the number of hits per domain is expressed by the scale factor Z, which at most is a factor of 2 larger than y (see above).

Eq. 31 allows for the calculation of the quantum yield ϕ as a function of y for different values of the parameter r. Curves of ϕ vs. log y for different values of r are plotted in
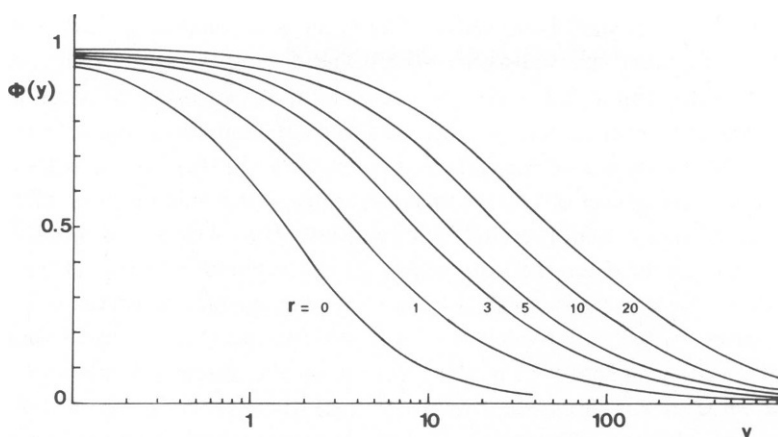
FIGURE 5 Calculated values of the fluorescence quantum yield $\phi(y, r)$ as a function of the number of hits per domain, y, for different values of the parameter r.

Fig. 5. In general, the curves differ from each other in shape and in position with respect to the abscissa. It should be noted that as the value of r increases, the curves drop off less steeply and are shifted to the right on the horizontal log y scale. This is due to the fact that the efficiency of annihilation decreases as the value of r increases. For $r > 20$, the curves have exactly the same shape as the one obtained in the Swenberg model (8). We conclude that it is possible to determine r from the shape of the quenching curve; if, in addition, the monomolecular decay rate K is known, the bimolecular annihilation rate γ can be calculated. This will be described in more detail below.

Additional information may be obtained from the quenching curves. Let X be the average number of excitons created per photosynthetic unit at $t = 0$. If there are d photosynthetic units per domain, the following relation is obtained:

$$y = dX. \tag{32}$$

After the value of r is determined by comparing the shapes of the experimentally determined quenching curves with those calculated theoretically (Fig. 5), a comparison of the position, with respect to the abscissa, of the experimental ϕ vs. log X and the theoretical ϕ vs. log y curves gives the value of d directly. It should be noted that d is related to the physical dimensions of the domains, i.e., the number of chlorophyll molecules per domain. We illustrate this by an example.

Let us consider a system consisting of three isolated units. Suppose that at $t = 0$ one exciton is created in each of the units. Because the units are isolated there is no exciton-exciton annihilation and the quantum yield is ϕ_0. Let us now suppose that these three units are connected and that the excitons can move freely within all of the units. These three units thus form a single domain in which three excitons are created at $t = 0$. Singlet-singlet annihilations may now occur and the yield will be less than ϕ_0 (the yield will be equal to $\phi_0/3$ if γ is very large, i.e., if $r = 0$). It is due to this type of effect only, in which the reaction centers play no role, and which depends only on the number of chlorophyll molecules over which the excitons can freely range, that the value of d can be evaluated.

At this point it is appropriate to note the difference between the physical size of the do-

mains and the functional size of the PSUs. The latter is defined as the number of chloro-phyll molecules per functional reaction center. The difference can be illustrated by using our example of three connected units. We suppose that two different situations are possible, one in which the three centers are functional (i.e., are capable of annihilating excitons), and the other where only one of the centers is functional. In these two cases, d is the same, but r is not. If capture of excitons by the reaction centers is the only mode of monomolecular decay (i.e., not involving exciton-exciton annihilation), K as well as r diminish by a factor of 3 when two out of the three reaction centers do not act as quenchers. If the initial value of r is neither too large nor too small, the shapes of the quenching curves will be different in these two cases. If the initial value of r were close to zero, the curves would not differ from each other either in shape, or in the position on the abscissa in plots of ϕ vs. log y. If the initial value of r is large (the Swenberg case), the quenching curve will be slightly shifted to the left (lower values of log y). In this latter case, it is not possible to distinguish any changes in the functional or physical size of the PSU. This result is due to the fact that for large r, ϕ depends on the single parameter d/r.

We are now able to compare our fluorescence quenching model with the one proposed by Mauzerall (6, 7). With domains containing one reaction center, Mauzerall obtains the expression

$$\phi = \phi_0(1 - e^{-X})/X. \tag{33}$$

This formula is identical to the one we obtain for the particular case of $r = 0$ and $d = 1$. Nevertheless we will see below that our model is based on a different physical concept. Mauzerall has also examined the case in which the domains contain several traps and has derived the following equation, which in our notation is

$$\phi = \frac{\phi_0}{y} \sum_1^\infty d' P_n \left(1 - \left(\frac{d' - 1}{d'}\right)^n\right). \tag{34}$$

(We use y rather than x here to emphaszie the notion of a domain as consisting of an ensemble of chlorophyll molecules over which the excitons are capable of migrating. Furthermore, we use d' rather than d because in Mauzerall's theory the number of traps is not necessarily equal to the total number, d, of reaction centers). The nth Poisson distribution is given by P_n.

Eq. 34 can be simplified, because

$$P_n = (1/n!)y^n e^{-y}$$

and the summation over n gives:

$$\phi = \phi_0 \frac{1}{y/d'} [1 - \exp(-y/d')] \tag{35}$$

It is evident that ϕ depends only on the single parameter y/d'. This model thus leads to results different from ours with respect to two different points: (a) the curves of ϕ vs. log y all have the same shape, irrespective of the value of d'. They are nevertheless displaced along the abscissa for different values of d', and d' here plays the role of the pa-

rameter r in our theory; (b) analysis of the quenching curves provides information only about the ratio d/d'. No information on the size of the domains can be obtained, however.

This last point may be illustrated by using our example of three photosynthetic units. We take the case where all three reaction centers are functional, i.e., are capable of annihilating excitons. We can see immediately from Eq. 35 that the Mauzerall model is not capable of distinguishing between the case of isolated units ($d = d' = 1$) and the case where the units are connected ($d = d' = 3$).

By examining the shape of the quenching curves and using our model, it is possible to determine the physical size of the domains. Using the Mauzerall model, or the Swenberg model for that matter, it is possible only to determine the functional dimensions of the units, or the change in this dimension produced by some external variable.

There is, nevertheless, a similarity between the two theories. We have already pointed out that the parameter r defines both the shape and the position with respect to the abscissa log y of the quenching curves ϕ vs. log y (Fig. 5). The parameter d' is important only in determining the position of the curve with respect to the horizontal scale. If we neglect, for the moment, any differences in the shapes of the curves in Fig. 5, these two parameters, d' and r, play a similar role. However, the parameter r has a much more general significance than d because $r = 2K/\gamma$, r is proportional to d', as K depends on the number d' of active reaction centers. However, r takes into account all possible modes of unimolecular decay, including those variations in K not due solely to changes in d'.

The principal differences in the results obtained from the two models—shapes of the quenching curves, effect of the size of the domains—are due to the different physical hypotheses on which the two models are based. We recall that in our model the strong fluorescence quenching at high excitation intensities is due to singlet-singlet annihilations. It is because of these annihilations that we obtain information about the size of the domains in our model. The physical occurrence of this process does not depend on the reaction centers.

In the Mauzerall model, the quenching is due to the annihilation of excitons by reaction centers that have already captured one exciton. This type of quenching thus depends directly on the number of reaction centers present in the domains.

These differences in the physical hypotheses appear even in the case when the two models approach the same limit, giving rise to identical formulas for ϕ, namely, the case $r = 0$, $d = d' = 1$, units containing a single trap. In the Mauzerall theory, the fluorescence is emitted as long as the reaction center has not been hit by any exciton; one can say that if several excitons are present "only the first one can decay via fluorescence." In our model, there is a complete annihilation of excitons ($r = 0$ and thus $\gamma \rightarrow \infty$) as long as there is more than one exciton in a domain. One can say that out of several excitons in a domain, "only the last remaining exciton may decay via fluorescence."

Finally, we note that although the two theories are markedly different, one does not exclude the other. These two theories apply to different cases. Mauzerall has treated the fluorescence quenching produced by nanosecond laser pulse excitation. Due to the relatively long duration of this pulse, long-lived excited states can act as quenchers of singlets. It is possible that such long-lived quenchers are preferentially formed at the level of the reaction centers. In this work we have concerned ourselves only with the case of excitation by

picosecond laser pulses and have assumed that only the singlet excitons themselves can act as quenchers.

Analysis of Experimental Results

We use our previous experimental results (9), the most detailed data to date on fluorescence quenching as a function of the intensity of picosecond laser pulses at different temperatures. We compare theoretical curves of ϕ vs. log y with experimentally obtained curves ϕ vs. log X, where in both cases ϕ is normalized to unity in the low intensity limits. The fit of the theoretical and experimental curves involves two factors: (a) Superimposition of ϕ(theor) on ϕ(exp), which in principle defines the value of $r(=2\gamma/K)$, because the curves of different r vary in shape (this variation is small for all curves with $r > 5$). (b) By sliding the ϕ(exp) curves relative to the ϕ(theor) curve along the abscissa, the two curves can be made to coincide when $y = dX$. Because y is the calculated parameter of photon hits per domain, whereas X is the experimentally determined value of hits/PSU, the value of d, the number of PSUs per domain, can be calculated from such a superposition.

In reference 9, ϕ(exp) vs. X curves are given at four different temperatures, namely, 21°, 100°, 200°, and 300°K. Rather than fit each curve separately in the manner described above, we proceeded as follows:

(a) First, we ascertained that the ϕ(exp) vs. log X curves had similar shapes, regardless of the temperature. These curves differ from each other only by a horizontal displacement along the abscissa (log X).

(b) Because the shapes of the curves are the same at all four temperatures, we have plotted all of the data on the same graph (Fig. 6) and noted the position on the *relative* log X scale, for which $X = 1$ for each of the four temperatures.

(c) By sliding the theoretical curves of Fig. 5 plotted on a transparent cellophane sheet over those given in Fig. 6, the values of r may be determined.

(d) The position for which $X = 1$ along the abscissa in Fig. 6 is different for the four temperatures. The least amount of quenching for $X = 1$ occurs at 300°K, whereas the most quenching for $X = 1$ takes place at 21°K. The 100°K $X = 1$ points do not appear to follow this trend, i.e., the lower the temperature, the more efficient the quenching; whether or not this particular result is significant cannot be determined, and we shall refrain from commenting on this anomaly any further at this time.

(e) Variations in r as a function of temperature are expected if either γ and/or K vary with the temperature. Indeed, Hervo et al. (25) have observed little variation in the fluorescence decay time from 100–300°K ($K^{-1} \simeq 0.8$ ns) whereas $K^{-1} = 1.1$ ns at 23°K; these measurements were obtained by viewing the fluorescence at 680 nm, which corresponds to the emission from light harvesting and photosystem II chlorophyll a molecules (we note also that the fluorescence quenching data shown in Fig. 6 also pertains to the light harvesting pigment system [9]).

A superimposition of the theoretical curves shown in Fig. 5 on the experimental data in Fig. 6 demonstrates clearly that the $r = 0$ curves cannot account for the experimental results; this was already pointed out in reference 9. The best theoretical fits are obtained with the curves $r > 10$; however, because of the significant scatter in the experimental data, a fit of the $r = 5$ curves cannot be completely ruled out.
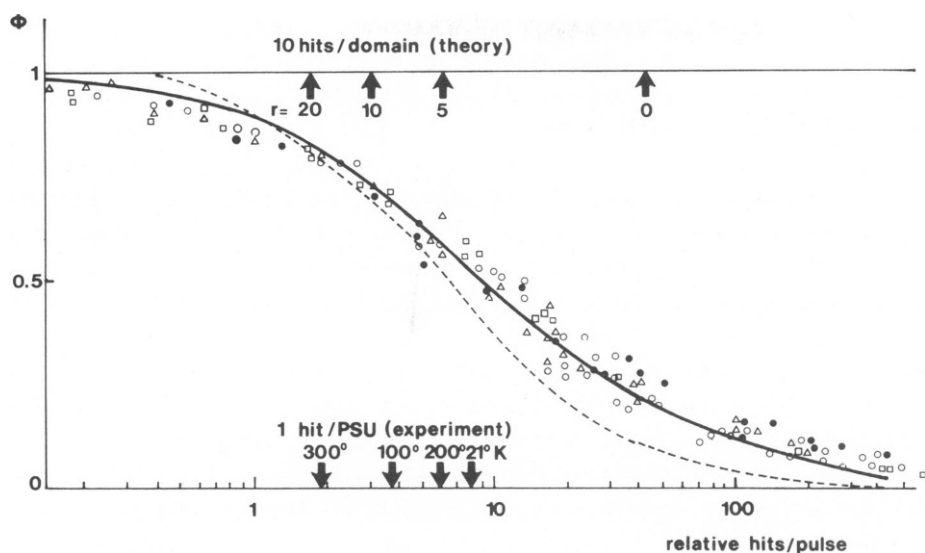
FIGURE 6 Comparison of calculated and experimental quantum yield curves. The data are taken from reference 9. The sets of data at four temperatures (21°, 100°, 200°, and 300°K) of the horizontal (photon hits per PSU) axes; the location of the 1 hit/PSU (1 PSU ~ 300 chlorophyll molecules) at the four different temperatures is indicated on the bottom of the figure. (Δ) 300°K; (o) 200 °K; (•) 100°K; and (□) 21°K. The solid line corresponds to the superimposition of the theoretically calculated curves (Fig. 5) on the experimental data; the solid line corresponds to the spread obtained by superimposing the $r = 5$, 10, and 20 curves. The dotted line represents the $r = 0$ case. A translation along the horizontal axis was required to obtain the superpositions shown; the points for which there are 10 hits/domain for each r curve are indicated on the top of the figure.

Even though r is expected to vary slightly with temperature, as pointed out above, these variations cannot be discerned because of the subtle differences between the different r curves when $r > 5$, and because of the scatter in the experimental data. However, it can be stated with a reasonable degree of confidence that all of the experimental data at all temperatures can be described by $r > 5$. Using Eq. 32 and the values of y (Fig. 5) and X (Fig. 6) for which the theoretical curves and the experimental data superimpose (a few theoretical curves, appropriately translated along the abscissa, are also shown in Fig. 6), values of d, the number of PSUs per domain, can be calculated. For temperatures below 200°K with the $r = 5$ curve, $d > 7$. At 300°K ($r = 5$), $d = 4$. However, as r may change with temperature, the values of d are probably the same at all temperatures. If the $r = 10$ curve is chosen, then $d > 12$ below 200°K, and $d = 7$ at 300°K. Furthermore, in Eq. 32 ξ was taken to be zero for simplicity. Because $0 < \xi < 1$, Eq. 32 should read $y = (1 + \xi)dX$ in the most general case. Thus, all minimum values of d calculated for $\xi = 0$ should be divided by two to take into account the fact that ξ may have a nonzero value and may be as large as unity.

In summary, therefore, the analysis of the quenching curves yields the following highly conservative values for the lower limits of r and d: $r > 5$ and $d > 2$ (at 300°K) and $d > 4$ (below 200°K).

These results indicate that each domain in the light harvesting system consists of more than two to four connected units (see also the work of Joliot [20, 26] and Mauzerall

[6, 7]). Thus, the picosecond laser pulse fluorescence experiments confirm that the motion of excitons within the light harvesting antenna pigment systems is a relatively free motion including several connected photosynthetic units. The diffusion length of the excitons thus may be limited by the lifetime of the excitons and not by some barrier between photosynthetic units.

When considered separately, only lower limits may be obtained for r and d. Nevertheless, it is possible to get a more accurate value of the ratio r/d. As a matter of fact, when r is large (and, for instance, when $r > 5$), the quantum yield ϕ is a function of Z/r (Eq. 22) as a consequence of r/d. Then, at room temperature, one may assert that $r/d = 5/2$, because $K^{-1} \simeq 0.8$ ns, $d\gamma = 10^9 \text{s}^{-1}$.

γ may be easily calculated if one supposes that the diffusion of excitons is a limiting process. In this case γ^{-1} is equal to the average time needed for two excitons to meet for the first time and thus $\gamma^{-1} = m/\nu L$, where m is the number of jumps performed by one exciton before reaching the other one in a domain, L is the rate of exciton transfer between two neighboring chlorophyll molecules, and ν is the number of nearest neighbors. Thus $L = m/d\nu \cdot 10^9 \text{s}^{-1}$.

For a planar square lattice $m/d\nu$ is about 100 (Montroll, 27), thus $L \simeq 10^{11}\text{s}^{-1}$.

Inasmuch as this value was calculated by assuming that the diffusion is a limiting process, it is actually the value of its lower limit. This indicates, as shown previously (17–19, 28), that the rate of exciton transfer in the photochemical apparatus is rather large.

SUMMARY AND CONCLUSIONS

The theory developed here can account for all of the experimental data on the fluorescence quantum yield and decay curves obtained in picosecond laser excitation experiments. The equations derived here to describe ϕ and $F(t)$ as a function of the pulse intensity are based on the Pauli master equation and on Poisson statistics. It is shown that the equations developed by Mauzerall (6, 7) and by Swenberg et al. (8) are similar to those obtained in the limiting case of $r = 0$ and $r = \infty$, respectively, of the general theory. Experimental quantum yield curves as a function of pulse intensity are better described in terms of $r > 0$ than in terms of the $r = 0$ theoretical limit. In principle, the value of $r = 2K/\gamma$ can be determined from the shape of $\phi(y)$ curves ($y = $ hits/domain), but in practice the shapes of these curves for all values of $r > 5$ are so similar that they are not easily distinguished from each other. By taking $r = 5$ as a lower limit, a minimum size of the photosynthetic domain can be estimated. Most probably, such a domain contains more than 2–4 PSU, where each unit is taken to consist of ~300 chlorophyll molecules. It is likely that the spatial extent of the diffusion of excitons in photosynthetic membranes is limited by their lifetime, rather than by some physical barrier encompassing one or more reaction centers.

The decay profiles of the fluorescence excited by picosecond pulses can be described by a sum of exponentials, all of them except the first containing the bimolecular annihilation rate constant γ as a parameter. Under certain specialized conditions involving the number of photon hits per domain, and the magnitude of the parameter r, the square root of time decay law observed experimentally by Porter and his co-workers (10) is obtained.

REFERENCES

1. BRETON, J., and N. E. GEACINTOV. 1976. Quenching of fluorescence of chlorophyll in vivo by long-lived excited states. *FEBS (Fed. Eur. Biochem. Soc.) Lett.* **69**:86–89.
2. GEACINTOV, N. E., and J. BRETON. 1977. Exciton annihilation in the two photosystems in chloroplasts at 100°K. *Biophys. J.* **17**:1–15.
3. GEACINTOV, N. E., J. BRETON, C. E. SWENBERG, A. J. CAMPILLO, R. C. HYER, and S. L. SHAPIRO. 1977. Picosecond and microsecond pulse laser studies of exciton quenching and exciton distribution in spinach chloroplasts at low temperatures. *Biochim. Biophys. Acta.* **461**:306–312.
4. CAMPILLO, A. J., R. C. HYER, T. G. MONGER, W. W. PARSON, and S. L. SHAPIRO. 1977. Light collection and harvesting processes in bacterial photosynthesis investigated on a picosecond timescale. *Proc. Natl. Acad. Sci. U.S.A.* **74**:1977–2001.
5. CAMPILLO, A. J., S. L. SHAPIRO, V. H. KOLLMAN, K. R. WINN, and R. C. HYER. 1977. Picosecond exciton annihilation in photosynthetic systems. *Biophys. J.* **16**:93–97.
6. MAUZERALL, D. 1976. Multiple excitations in photosynthetic systems. *Biophys. J.* **16**:87–91.
7. MAUZERALL, D. 1976. Fluorescence and multiple excitation in photosynthetic systems. *J. Phys. Chem.* **80**: 2306–2309.
8. SWENBERG, C. E., N. E. GEACINTOV, and M. POPE. 1976. Bimolecular quenching of excitons and fluoresence in the photosynthetic unit. *Biophys. J.* **16**:1447–1452.
9. GEACINTOV, N. E., J. BRETON, C. E. SWENBERG, and G. PAILLOTIN. 1977. A single pulse picosecond laser study of exciton dynamics in chloroplasts. *Photochem. Photobiol.* **26**:629–638.
10. PORTER, G., J. A. SYNOWIEC, and C. J. TREDWELL. 1977. Intensity effects on the fluorescence of in vivo chlorophyll. *Biochim. Biophys. Acta.* **459**:329–336.
11. BEDDARD, G. S., and G. PORTER. 1977. Excited state annihilation in the photosynthetic unit. *Biochim. Biophys. Acta.* **462**:63–72.
12. SEARLE, G. F. W., J. BARBER, L. HARRIS, G. PORTER, and C. J. TREDWELL. 1977. Picosecond laser study of fluorescence lifetimes in spinach chloroplast photosystem I and photosystem II preparations. *Biochim. Biophys. Acta.* **459**:390–401.
13. HARRIS. L., G. PORTER, J. A. SYNOWIEC, C. J. TREDWELL, and J. BARBER. 1976. Fluorescence lifetimes of *Chlorella pyrenoidosa. Biochim. Biophys. Acta.* **449**:329–339.
14. BARBER, J., G. F. W. SEARLE, and C. J. TREDWELL. 1978. Picosecond time-resolved study of $MgCl_2$-induced chlorophyll fluorescence yield changes from chloroplasts. *Biochim. Biophys. Acta.* **501**:174–182.
15. KENKRE, V. M., and R. S. KNOX. 1974. Generalized-master-equation theory in excitation transfer. *Phys. Rev.* **B9**:5279–5286.
16. PAILLOTIN, G. 1972. Transport and capture of electronic excitation energy in the photosynthetic apparatus. *J. Theor. Biol.* **36**:223–235.
17. ROBINSON, G. W. 1967. Excitation transfer and trapping photosynthesis. *Brookhaven Symp. Biol.* **19**:16–48.
18. PAILLOTIN, G. 1976. Capture frequency of excitations and energy transfer between photosynthetic units in the photosystem II. *J. Theor. Biol.* **58**:219–235.
19. PAILLOTIN, G. 1976. Movement of excitations in the photosynthetic domains of photosystem II. *J. Theor. Biol.* **58**:237–252.
20. JOLIOT, A., and P. JOLIOT. 1964. Etude cinétique de la réaction photochimique libérant l'oxygène au cours de la photosynthèse, *C.R. Acad. Sci. Paris.* **258**:4622–4625.
21. CAMPILLO, A. J., V. H. KOLLMAN, and S. L. SHAPIRO. 1976. Intensity dependence of the fluorescence lifetime of in vivo chlorophyll excited by a picosecond light pulse. *Science (Wash. D.C.).* **193**:227–229.
22. KNOX, R. S. 1977. Photosynthetic efficiency and exciton transfer and trapping. *In* Primary Processes of Photosynthesis. Vol. 2. J. Barber, editor. Elsevier, Amsterdam. 55–97.
23. SWENBERG, C. E., and N. E. GEACINTOV. 1973. Exciton interactions in organic solids. *In* Organic Molecular Photophysics. J. B. Birks, editor. J. Wiley & Sons, Ltd, Chichester, Sussex, England. 489–564.
24. FÖRSTER, T. 1949. Experimentelle und theoretische Untersuchung des zwischenmolekularen Ubergang von Elektronenanregungsenergie. *Z. Naturforsch.* 4a:321–327.

25. HERVO, G., G. PAILLOTIN, J. THIERY, and G. BREUZE. 1975. Détermination de différentes durées de vie de fluorescence manifestées par la chlorophylle a *in vivo, J. Chim. Phys. Physicochim. Biol.* **6:**761–766.

26. JOLIOT, P., P. BENNOUN, and A. JOLIOT. 1972. New evidence supporting energy transfer between photosynthetic units. *Biochim. Biophys. Acta.* **305:**317–328.

27. MONTROLL, E. W. 1969. Random walks on lattices. III. Calculation of first passage times with application to exciton trapping on photosynthetic units. *J. Math. Phys. (Cambridge, Mass.).* **10:**753–765.

28. PEARLSTEIN, R. M. 1967. Migration and trapping of excitation quanta in photosynthetic units. *Brookhaven Symp. Biol.* **19:**8–15.

APPENDIX

General Solution of the Pauli Master Equation

In this section we discuss the details of solving Eq. 10:

$$\frac{dp_i(n,t)}{dt} = K(i+1)p_{i+1}(n,t) + \gamma^{(1)} \frac{i(i+1)}{2} p_{i+1}(n,t) + \gamma^{(2)} \frac{(i+1)(i+2)}{2} p_{i+2}(n,t)$$

$$-\left(Ki + \gamma^{(1)} \frac{i(i-1)}{2} + \gamma^{(2)} \frac{i(i-1)}{2}\right)p_i(n,t). \quad (10)$$

The general solution of this Pauli equation can be obtained by using the generating function method. We define

$$Z_n(n,t) = \sum_{i=0}^{n} (x^i - 1)p_i(n,t). \quad (A1)$$

Furthermore, we introduce the following Laplace transforms:

$$\tilde{Z}_n(x,s) = \int_0^\infty e^{-st} Z_n(x,t)\,dt$$

$$\tilde{P}_{ni}(s) = \int_0^\infty e^{-st} p_i(n,t)\,dt. \quad (A2)$$

In addition, it is useful to define the following symbols:

$$\gamma = \gamma^{(1)} + \gamma^{(2)} \qquad r = 2K/\gamma \qquad \xi = \gamma^{(2)}/\gamma. \quad (A3)$$

With the appropriate mathematical manipulations, it can be shown that Eq. 10 can be recast in the form:

$$r(1-x)\frac{\partial \tilde{Z}_n(x,s)}{\partial x} + (x+\xi)(1-x)\frac{\partial^2 \tilde{Z}_n(x,s)}{\partial x^2} = \frac{2}{\gamma}(1 - x^n + s\tilde{Z}_n(x,s)). \quad (A4)$$

The function $\tilde{Z}_n(x,0)$ obtained for $s = 0$ is a solution of the equation:

$$r(1-x)\frac{\partial \tilde{Z}_n(x,0)}{\partial x} + (x+\xi)(1-x)\frac{\partial^2 \tilde{Z}_n(x,0)}{\partial x^2} = \frac{2}{\gamma}(1 - x^n). \quad (A5)$$

We replace $\tilde{Z}_n(x,s)$ on the right-hand side of Eq. A-4 by the following expression, obtained from Eqs. A1 and A2:

$$\tilde{Z}_n(x,s) = \sum_{i=0}^{n} (x^i - 1)\tilde{P}_{ni}(s). \quad (A6)$$

With this substitution, $\tilde{Z}_n(x, s)$ may be calculated using Eq. A5, and one obtains:

$$\tilde{Z}_n(x,s) = \tilde{Z}_n(x,0) - s \sum_{i=0}^{n} \tilde{P}_{ni}(s) \tilde{Z}_i(x,0) \qquad (A7)$$

Because $\tilde{P}_{nm}(s)$ is the x^m term in $\tilde{Z}_n(x,s)$, it follows that

$$\tilde{P}_{nm}(s) = \tilde{P}_{nm}(0) - s \sum_{i=m}^{n} \tilde{P}_{ni}(s) \tilde{P}_{im}(0). \qquad (A8)$$

By successive iteration, this equation may be rewritten as

$$\tilde{P}_{nm}(s) = \tilde{P}_{nm}(0) - s \sum_{i=m}^{n} \tilde{P}_{ni}(0) \tilde{P}_{im}(0) + s^2 \sum_{i=m}^{n} \sum_{j=i}^{n} \tilde{P}_{nj}(0) \tilde{P}_{ji}(0) \tilde{P}_{im}(0)$$
$$+ \dots. \qquad (A9)$$

We thus replace $\tilde{P}_{ni}(s)$ in Eq. A7 by its equivalent calculated from Eq. A9, and obtain:

$$\tilde{Z}_n(x,s) = \tilde{Z}_n(x,0) - s \sum_{i=0}^{n} \tilde{P}_{ni}(0) \tilde{Z}_i(x,0) + s^2 \sum_{i=0}^{n} \sum_{j=i}^{n} \tilde{P}_{nj}(0) \tilde{P}_{ji}(0) \tilde{Z}_i(x,0)$$
$$- s^3 \sum_{i=0}^{n} \sum_{j=i}^{n} \sum_{k=j}^{n} \tilde{P}_{nk}(0) \tilde{P}_{kj}(0) \tilde{P}_{ji}(0) \tilde{Z}_i(x,0)$$
$$+ \dots. \qquad (A10)$$

In the summation on the right-hand side of Eq. A10, the indices $i, j, k \dots$ appear in decreasing order $i \leq j \leq k \text{--------}$. By a simple permutation of summations these indices can be recast in an increasing order, and one obtains:

$$\tilde{Z}_n(x,s) = \tilde{Z}_n(x,0) - s \sum_{i=0}^{n} \tilde{P}_{ni}(0) \tilde{Z}_i(x,0) + s^2 \sum_{i=0}^{n} \sum_{j=0}^{i} \tilde{P}_{ni}(0) \tilde{P}_{ij}(0) \tilde{Z}_j(x,0)$$
$$- s^3 \sum_{i=0}^{n} \sum_{j=0}^{i} \sum_{k=0}^{j} \tilde{P}_{ni}(0) \tilde{P}_{ij}(0) \tilde{P}_{jk}(0) \tilde{Z}_k(x,0) + \cdots$$

Thus,

$$\tilde{Z}_n(x,s) = \tilde{Z}_n(x,0) - s \sum_{i=0}^{n} \tilde{P}_{ni}(0) \tilde{Z}_i(x,s). \qquad (A11)$$

By replacing $\tilde{Z}_n(x, 0)$ in this equation by its equivalent obtained from (A6), one obtains:

$$\tilde{Z}_n(x,s) = \sum_{i=0}^{n} \tilde{P}_{ni}(0)((x^i - 1) - s \tilde{Z}_i(x,s)). \qquad (A12)$$

We now turn to a consideration of the time-dependent functions $Z_n(x, t)$. For $t = 0$, it follows from Eq. A1 that

$$Z_n(x,0) = x^n - 1.$$

Thus, according to Eq. A12 we can write:

$$Z(x, t) = -\frac{d}{dt} \sum_{i=0}^{n} \tilde{P}_{ni}(0) Z_i(x, t). \qquad (A13)$$

By introducing the matrix $\tilde{\mathbb{P}}(0)$ (whose elements are $\tilde{P}_{nm}(0)$) and the column vector $Z(x, t)$ defined by elements $Z_n(x, t)$, this equation may be written as

$$Z_n(x, t) = -\frac{d}{dt} (\tilde{\mathbb{P}}(0) Z(x, t))$$

and, in addition,

$$\tilde{\mathbb{P}}^{-1}(0) Z(x, t) = -\frac{d}{dt} Z(x, t). \qquad (A14)$$

Multiplying Eq. 10 by $(\tilde{\mathbb{P}}^{-1}(0))_{mn}$ and summing over n, we obtain:

$$(\tilde{\mathbb{P}}^{-1}(0))_{mn} = \frac{\gamma}{2} (\delta_{mn} m(m + r - 1) - \delta_{m,n+1} m(r + (m - 1)(1 - \xi))$$

$$- \delta_{m,n+2} m(m - 1)\xi). \qquad (A15)$$

This equation, in conjunction with Eq. A14, gives a difference equation for $Z_n(x, t)$:

$$\frac{2}{\gamma} \frac{d}{dt} Z_n(x, t) = -(n(r + n - 1)(Z_n(x, t) - Z_{n-1}(n, t))$$

$$+ \xi n(n - 1)(Z_{n-1}(x, t) - Z_{n-2}(x, t))). \qquad (A16)$$

The fluorescence intensity $F_n(t)$ for a given domain containing n excitons at $t = 0$ is given by

$$F_n(t) = \frac{1}{n} \sum_{i=0}^{n} i p_i(n, t) = \frac{1}{n} \left. \frac{\partial Z_n(x, t)}{\partial x} \right|_{x=1} \qquad (A17)$$

The macroscopic fluorescence intensity is given by the equation (cf. Eq. 15)

$$F(t) = \sum_{n=1}^{\infty} \frac{y^{n-1} e^{-y}}{(n - 1)!} F_n(t) \qquad (A18)$$

Setting $Z = y(1 + \xi)$ and using Eqs. A16, A17, and A18, the following relation is obtained:

$$-\frac{2}{\gamma} \frac{\partial F}{\partial t} = (r + Z)F + Z(r + 2 + Z) \frac{\partial F}{\partial Z} + Z^2 \frac{\partial^2 F}{\partial Z^2}. \qquad (A19)$$

Introducing the Laplace transform

$$\tilde{F}(Z, s) = \int_0^{\infty} e^{-st} F(Z, t) dt \qquad (A20)$$

and using Eq. A19 gives

$$\tilde{F}(Z,s) = \frac{2}{\gamma} \sum_{k=0}^{\infty} \frac{(-1)^k Z^k k!}{(2s/\gamma + (k+1)(k+r))(2s/\gamma + k(k-1+r))\ldots(2s/\gamma + r)}$$

$$= \frac{2}{\gamma} \sum_{k=0}^{\infty} (-1)^k Z^k k! \left\{ \prod_{j=0}^{k} \frac{1}{(2s/\gamma + (j+1)(j+r))} \right\}. \tag{A21}$$

From A21 it follows that $\tilde{F}(Z,s)$ is a product of convolution of exponential decays; each exponential mode (rate constant of the exponential mode) is equal to

$$\frac{\gamma}{2}(j+1)(j+r) = \gamma \frac{j(j+1)}{2} + K(j+1). \tag{A22}$$

This rate is equal to the rate of disappearance of a $(j+1)$ exciton state. So within a first approximation Eq. A21 can be generalized by explicitly taking into account a dependence of γ on i, i.e., $\gamma \rightarrow \gamma_i$. $\tilde{F}(Z,s)$ is then given by

$$\tilde{F}(Z,s) \simeq \frac{2}{\gamma} \sum_{k=0}^{\infty} (-1)^k Z^k k! \left\{ \prod_{j=0}^{k} \frac{1}{(2s/\gamma_{i+1}) + (j+1)(j+2K/\gamma_{i+1})} \right\}. \tag{A23}$$